Kinetic Analysis of the Coding Properties of O^6-Methylguanine in DNA: The Crucial Role of the Conformation of the Phosphodiester Bond†

Hwee-Boon Tan, Peter F. Swann,* and Edwin M. Chance

Cancer Research Campaign Nitrosamine-induced Cancer Group, Department of Biochemistry and Molecular Biology, University College London, Gower Street, London WC1E 6BT, United Kingdom

Received January 27, 1994®

ABSTRACT: Production by *N*-nitroso compounds of O^6-alkylguanine (O^6-alkylG) in DNA directs the misincorporation of thymine during DNA replication, leading to G:C to A:T transition mutations, despite the fact that DNA containing O^6-alkylG:T base pairs is less stable than that containing O^6-alkylG:C pairs. We have examined the kinetics of incorporation by Klenow fragment (KF) of *Escherichia coli* DNA polymerase I of thymine (T) and of cytosine (C) opposite O^6-MeG in the template DNA strand. Both T and C were incorporated opposite O^6-MeG much slower than nucleotides forming regular A:T or G:C base pairs. Using various concentrations of dTTP, dCTP, or their phosphorothioate (S_p)-dNTPαS analogues, or a mixture of dTTP and dCTP, the progress of incorporation of a single nucleotide in a single catalytic cycle of a preformed KF–DNA complex was measured (pre-steady-state kinetics). The results were consistent with the kinetic scheme (Kuchta, R. D., Benkovic, P., & Benkovic, S. J. (1988) *Biochemistry 27,* 6716–6725): (1) binding of dNTP to polymerase–DNA; (2) conformational change in polymerase; (3) formation of phosphodiester between the dNTP and the 3′-OH of the primer; (4) conformational change of polymerase; (5) release of pyrophosphate. The results were analyzed mathematically to identify the steps at which the rate constants differ significantly between the incorporation of T and C. The only significant difference was the 5-fold difference in the rates of formation of the phosphodiester bond (for dTTP, $k_{forward}$ = 3.9 s^{-1} and k_{back} = 1.9 s^{-1}; for dCTP, $k_{forward}$ = 0.7 s^{-1} and k_{back} = 0.9 s^{-1}). These pre-steady-state progress curves were biphasic with a rapid initial burst followed by an apparently steady-state rise. Deconvolution of these curves gave direct evidence for the importance of the conformational change after polymerization by showing that the curves represented the sum of the rapid accumulation of the product of step 3 followed by the slow conversion of that to the product of step 5 (because of the rapidity of the release of pyrophosphate there was no significant accumulation of the product of step 4). The equilibrium constants for each step suggest that the greatest change in the Gibbs free energy occurs at the conformational change after polymerization and that while the formation of the phosphodiester bond to T is slightly exothermic, that to C is slightly endothermic. K_m values obtained from Michaelis–Menten analysis of the initial rates of pre-steady-state polymerization were 27.6 and 26.4 μM for T and C, respectively. These calculated rate constants closely predicted the progress of independently determined steady-state experiments (i.e. excess DNA over KF) and also predicted the measured K_m. The incorporation of the nucleotide following C in an O^6-MeG:C pair was much slower than that following T in an O^6-MeG:T pair. Structural data has shown that the T:O^6-alkylG base pair retains the Watson–Crick configuration (with N1 of the purine juxtaposed to N3 of the pyrimidine), whereas the C:O^6-alkylG base pair is a wobble base pair. The C:O^6-alkylG base pair has distorted phosphodiester links both 3′ and 5′ to the C (Kalnik, M. W., Li, B. F. L., Swann, P. F., & Patel, D. J. (1989) *Biochemistry 28,* 6170–6181 and 6182–6192). The slow incorporation of C opposite O^6-MeG and of the next correct nucleotide following the incorporation of C can be ascribed to the stereochemical problems encountered when forming these distorted phosphodiester links.

The promutagenic alkylated bases O^6-alkylguanine (Loveless, 1969) and O^4-alkylthymine (Lawley et al., 1973) which the *N*-nitroso compounds produce during their reaction with DNA play the most important role in the carcinogenic action of these compounds, possibly through the induction of mutations in protooncogenes (Zarbl et al., 1985; Sukumar, 1990; Kumar et al., 1990). The presence of O^6-alkylguanine in DNA decreases the rate of DNA synthesis (Snow et al., 1984) and directs the misincorporation of thymine on replication of the alkylated DNA (Loveless, 1969; reviewed by Saffhill et al. (1985)). It has been generally accepted that misincorporation of thymine (T) opposite O^6-alkylguanine is the result of the formation of a more stable base pair between O^6-alkylguanine and thymine than between O^6-alkylguanine and cytosine (C), but melting studies of DNA duplexes containing O^6-methylguanine (O^6-MeG) show that O^6-MeG:T base pairs are energetically less stable than O^6-MeG:C (Gaffney & Jones, 1989), and NMR studies of DNA duplexes containing either O^6-methylguanine (Patel et al., 1986a,b; Goswami et al., 1993) or O^6-ethylguanine (Kalnik et al., 1989a,b) show that the O^6-alkylG:T pair is less H-bonded than the O^6-alkylG:C pair. Thus O^6-alkylguanine like 2-aminopurine (Mhaskar & Goodman, 1984) and xanthine (Eritja et al., 1986) directs the incorporation of its less favored partner. The objective of this work was to examine this paradox in the hope that its resolution might add to our knowledge of the underlying factors in DNA replication as well as throw light on the mechanism of action of the carcinogenic nitrosamines.

† This work, which is supported by the Cancer Research Campaign, is dedicated to Prof. Rolf Preussmann with our best wishes for his 65th birthday.

* To whom correspondence should be addressed.

® Abstract published in *Advance ACS Abstracts,* April 15, 1994.

0006-2960/94/0433-5335$04.50/0

Reaction	Rate Constants	
$E + D \rightleftharpoons E.D$	k_1 k_{-1}	Enzyme binds to DNA (D) to form E.D complex
$E.D + N \rightleftharpoons E.D.N$	k_2 k_{-2}	E.D complex binds dNTP (N)
$E.D.N \rightleftharpoons E^*.D.N$	k_3 k_{-3}	Enzyme undergoes conformational change to E*
$E^*.D.N \rightleftharpoons E^*.D_{n+1}.PPi$	k_4 k_{-4}	Phosphodiester bond is formed
$E^*.D_{n+1}.PPi \rightleftharpoons E.D_{n+1}.PPi$	k_5 k_{-5}	Second conformational change
$E.D_{n+1}.PPi \rightleftharpoons E.D_{n+1} + PPi$	k_6 k_{-6}	Pyrophosphate is released
$E.D_{n+1} \rightleftharpoons E + D_{n+1}$	k_7 k_{-7}	Enzyme dissociates from DNA
$E.D_{n+1} \rightarrow E.D + NMP$	k_{exo}	Exonuclease action

FIGURE 1: Kinetic scheme for the incorporation of a single nucleotide by Klenow fragment from Kuchta et al. (1988).

Replication of DNA is catalyzed by DNA polymerases with speed and high fidelity; for example, 1000 bases/s are added in *Escherichia coli* with an error frequency of only 10^{-8} to 10^{-10} per nucleotide incorporated (Englisch et al., 1985). The question of how DNA polymerases achieve this remarkably high level of fidelity has attracted much attention, and many models have been put forward to explain it (Loeb & Reyland, 1987; Radman & Wagner, 1988; reviewed by Echols & Goodman, 1991; Kunkel, 1992; Johnson, 1993). Some studies conducted under steady-state conditions, that is under conditions where there is a great excess of DNA over polymerase, demonstrated huge differences in the values of K_m but small differences in V_{max} between the incorporation of correct and incorrect base pairs (Boosalis et al., 1987; Preston et al., 1988; Boosalis et al., 1989) and thus led to the conclusion that K_m discrimination plays an important role in achieving fidelity during DNA replication. This theory was carried further by attributing these K_m differences to the free energy of binding of the nucleotide triphosphate to the active site of the polymerase (Boosalis et al., 1987; Petruska et al., 1988). Other studies have shown that V_{max} as well as K_m can be used to discriminate against the incorporation of mismatched nucleotides (El-Deiry et al., 1988). Similar studies of the incorporation of thymine and cytosine opposite O^6-methylguanine in the template DNA strand have been carried out by Singer et al. (1989) and Dosanjh et al. (1991), using techniques developed by Goodman and his colleagues. The results of these studies were quite complex. In every case, cytosine and thymine were incorporated opposite O^6-methylguanine with the same apparent V_{max}, although the actual V_{max} depended on the primer–template used possibly because the conformation of O^6-alkylguanine:N base pairs depends on the flanking sequence (Bishop & Moschel, 1991; Georgiadis et al., 1991). The apparent K_m also differed with some but not all primer–templates. More recently, Dosanjh et al. (1993) have suggested that O^6-methylguanine in DNA may have two conformations and that nucleotides are incorporated opposite one conformation more rapidly than opposite the other.

This unsatisfactory situation has been clarified by work primarily from the laboratories of Benkovic and of Johnson. They have carried out pre-steady-state studies (reviewed by Carroll and Benkovic (1990) and Johnson (1993)), in which the enzyme–DNA complex was preformed, the reaction begun by the addition of dNTPs and magnesium ions, and a single catalytic cycle of the enzyme followed, using either Klenow fragment of *E. coli* DNA polymerase I (Kuchta et al., 1987; 1988) or T7 DNA polymerase (Patel et al., 1991). Taken with related steady-state experiments (Kuchta et al., 1987; Kuchta et al., 1988; Wong et al., 1991), these studies have shown that addition of a single nucleotide to a pre-existing enzyme–DNA complex involves five kinetically discernable steps (Figure 1, steps 2–6). In the incorporation of a correctly paired nucleotide, the rate-limiting step is the conformational change (step 3 in Figure 1) rather than the formation of the chemical bond (Mizrahi et al., 1985; Kuchta et al., 1987; Patel et al., 1991).

In this paper, we have carried out an analysis of DNA synthesis on templates containing O^6-methylguanine using steady-state and pre-steady-state methods with Klenow fragment of *E. coli* DNA polymerase I. Klenow fragment was the enzyme of choice for several reasons. First of all, it is a simple peptide which does not require accessory proteins, the cloned gene has been expressed to yield very pure enzyme, and it has a high fidelity. Second, results with it could be compared with results of previous studies on the incorporation of mismatched nucleotides. Third, many detailed structural studies have been carried out on it, including X-ray crystallography (Ollis et al., 1985; Beese & Steitz, 1991; Beese et al., 1993), allowing kinetic data to be related to structural data. The results of our experiments have been analyzed by detailed mathematical analysis to identify at which step the rate constants differ between the incorporation of thymine and cytosine and thus lead to the preferential incorporation of thymine opposite O^6-methylguanine. This analysis shows that the only significant change is in the rate of formation of the phosphodiester bond itself and that there is no significant difference between incorporation of T and C in any of the other rate constants in Figure 1. The structure of base pairs involving O^6-alkylguanine has been studied by X-ray crystallography (Ginell et al., 1990; Leonard et al., 1990; Sriram et al., 1992) and by NMR. NMR has shown that the O^6-alkylguanine:T base pair has the normal Watson–Crick conformation with N1 of the purine juxtaposed to N3 of the pyrimidine (Patel et al., 1986a,b; Kalnik et al., 1989a,b), although with a greater than normal distance and possibly a water molecule between the two bases (Goswami et al., 1993). On the other hand, the O^6-alkylguanine:C base pair adopts a wobble conformation with H-bonds between N1 of the purine and the 4-amino group of C, and between the 2-amino group of the purine and N3 of C. In the ^{31}P NMR spectrum, one sees large changes of the chemical shift of the phosphodiesters both 3′ and 5′ to the C in the C:O^6-ethylguanine base pair in DNA, indicating significant changes in the conformation of these phosphodiesters (Kalnik et al., 1989a,b). The observation that the difference between the incorporation of T and of C by Klenow fragment is the slower formation of the phosphodiester bond suggests that the conformation of the phosphodiesters is a crucial factor which militates against incorporation of C.

MATERIALS AND METHODS

Enzymes and Nucleotides. T4 polynucleotide kinase was obtained from Amersham International, and snake venom phosphodiesterase (*Crotalus durissus*) and alkaline phosphatase were obtained from Boehringer Mannheim. FPLC-pure cloned Klenow fragment (1 unit = 2 pmol; 1 unit catalyzes the incorporation of 10 nmol of total deoxynucleotide into acid-insoluble product in 30 min at 37 °C with poly(dA-dT)·poly(dA-dT) as template), 2′-deoxynucleoside 5′-triphosphates (ultrapure grade), and the *S*-stereoisomers of 2′-deoxynucleoside 5′-*O*-(1-thiotriphosphate), [(S_p)-dNTPαS], were from Pharmacia. [γ-^{32}P]ATP was from New England Nuclear.

Synthesis of the DNA Primer–Templates. The sequences of the primer–templates used in this study are given in Table 1. Chemicals for oligodeoxynucleotide synthesis were obtained from Cruachem Ltd. (Glasgow, Scotland). The oligomers

Table 1: Primer–Template Duplexes[a]

Duplex A	5'ATCCGATAG 3'TAGGCTATC$_{meG}$TCATTCTCGC
Duplex B	5'ATCCGATAGT 3'TAGGCTATC$_{meG}$TCATTCTCGC
Duplex C	5'ATCCGATAGC 3'TAGGCTATC$_{meG}$TCATTCTCGC
Duplex D	5'ATCCGATAGT 3'TAGGCTATCAGTATTCTCGC

[a] Duplex A was used for studies of incorporation of cytosine or thymine opposite O^6-methylguanine. Duplexes B–D were used to measure the rates of 3′ → 5′ exonuclease activity and the addition of the next correct nucleotide.

containing only the naturally occurring bases were synthesized using solid-phase 2-cyanoethyl phosphoramidite chemistry. Oligomers containing O^6-methylguanine were synthesized according to the method of Smith et al. (1990) using phosphoramidite chemistry on a Cruachem System 200 A automated DNA synthesizer. All oligodeoxynucleotides were partially purified on a Nensorb Prep cartridge (DuPont) and then further purified by ion-exchange chromatography using a Mono Q HR 5-5 column (Pharmacia). The lengths of the oligomers were checked by electrophoresis on a 20% denaturing polyacrylamide gel against an oligo-dT ladder (Bethesda Research Ltd.). The purity of each oligodeoxynucleotide was determined by enzymic digestion with snake venom phosphodiesterase and alkaline phosphatase to nucleosides, chromatographic separation of the resulting nucleosides, and comparison of the integrated areas of the UV-absorbing peaks with those of a standard mixture of nucleosides (Graves et al., 1989).

^{32}P 5′-End-Labeling of Oligodeoxynucleotide Primers. The primers were 5′-end-labeled by incubating in 50 mM Tris·HCl (pH 7.4), 5 mM dithiothreitol, 1 mM spermidine, 10 mM $MgCl_2$, 10 units of T4 polynucleotide kinase, 1 nmol of primer DNA, and 50 μCi of [γ-^{32}P]ATP (3000 Ci/mmol) in a total volume of 10 μL at 37 °C. After 30 min, the reaction was terminated by heating to 70 °C for 2 min.

Annealing Oligodeoxynucleotide Primer–Templates. The ^{32}P-labeled primers were mixed with the complementary template DNA (to give a final DNA duplex concentration of 10 μM) in a solution containing 50 mM Tris·HCl (pH 7.4) and 5 mM $MgCl_2$ and annealed by heating the solution to 80 °C for 2 min and then allowing it to cool to room temperature over a period of 2–3 h. To ensure that all the primer would be in double-stranded DNA, 20% excess of the template strand was added.

Measurement of 3′ → 5′ Exonuclease Activity. The rate of removal of nucleotides at the 3′-terminus of the primer by the 3′ → 5′ exonuclease activity of Klenow fragment was measured by incubating at 30 °C 0.05 μM primer–template and 0.06 μM Klenow fragment in 50 mM Tris·HCl (pH 7.4) and 5 mM $MgCl_2$. After time intervals of 1–18 min, an aliquot was quenched into denaturing gel loading buffer (0.05% w/v bromophenol blue and 0.05% w/v xylene cyanole in formamide) and the products of exonuclease activity were separated by the electrophoretic method described below.

Steady-State Incorporation of Thymine or Cytosine opposite O^6-Methylguanine in the Template Strand. A solution containing 20 μM dNTP, 1 μM primer–template, 0.1 μM Klenow fragment, 50 mM Tris·HCl (pH 7.4), and 5 mM $MgCl_2$ was incubated at 30 °C for 30–420 s. The reaction was quenched into denaturing gel loading buffer (0.05% w/v bromophenol blue and 0.05% w/v xylene cyanole in formamide). The amount of primer elongated was measured as described below.

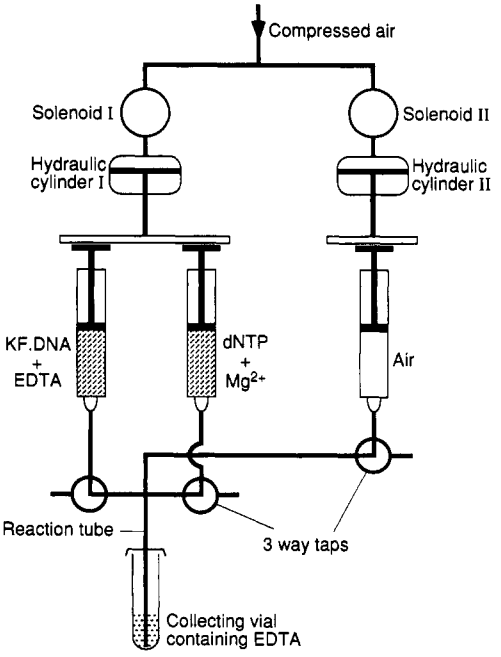

FIGURE 2: Rapid quench apparatus used for the pre-steady-state studies.

Pre-Steady-State Incorporation of Thymine or Cytosine opposite O^6-Methylguanine. The rapid-quench apparatus (Figure 2) is based on a design by Fersht (1985). The reaction was initiated by mixing reactants A and B: 40 μL of each reactant was drawn from each reservoir into syringes A and B, respectively (Hamilton gas-tight syringes, 100-μL capacity) using a three-way valve (Hamilton HVP valve, "T" housing with 90° plug). On the first signal from the timer, the contents of syringes A and B were discharged through a four-way connector (Chromatronix) into the reaction tube. On the second signal, 200 μL of air contained in syringe C (Hamilton gas-tight syringe, 500-μL capacity) blew the reaction mix into the quench solution (0.3 M EDTA). The length of the reaction tube was carefully measured so that it was just long enough to hold the reaction mixture. The syringe plungers were driven by two hydraulic cylinders (Schrader Bellows Model B3451 A, 1-in. stroke, 1-in. bore); plungers from syringes A and B were driven by hydraulic cylinder I, and the plunger from syringe C was driven by hydraulic cylinder II. The compressed-air supply (50 psi) driving these hydraulic cylinders was controlled by two Schrader solenoid valves Type LB 43323 SA (obtained from Darenth Automation, Croydon, Surrey, England) triggered by a home-made timer.

To measure the rate of incorporation of cytosine or thymine opposite O^6-methylguanine in the template strand, reservoir A was filled with 0.20 μM DNA primer–template, 0.24 μM Klenow fragment, 2.5 mM EDTA, and 50 mM Tris·HCl (pH 7.4) and reservoir B was filled with 10–160 μM dTTP or dCTP, 12.5 mM $MgCl_2$, and 50 mM Tris·HCl (pH 7.4). Reagent A (40 μL) was mixed with 40 μL of reagent B at room temperature, and after a time interval between 200 ms and 5 s (for dTTP) or 1 and 10 s (for dCTP), the reaction was quenched into 40 μL of 0.3 M EDTA (pH 7.4). The elongation of the primer was measured as described below.

To measure the rate of incorporation of the *S*-stereoisomer of the 2′-deoxynucleoside 5′-*O*-(1-thiotriphosphates), (S_p)-dTTPαS or (S_p)-dCTPαS, opposite O^6-methylguanine in the template strand, reservoir B was filled with 80 μM dNTPαS in a solution containing 12.5 mM $MgCl_2$ and 50 mM Tris·HCl.

To measure the incorporation of thymine and cytosine opposite O^6-methylguanine in the template strand when the enzyme–DNA complex was incubated with a mixture of dTTP and dCTP, reservoir B was filled with either 40 μM dTTP + 40 μM dCTP or 40 μM dTTP + 160 μM dCTP, in a solution containing 12.5 mM $MgCl_2$ and 50 mM Tris·HCl. In these competition experiments, the primer elongated by addition of T could be separated from that elongated by C (and from primer which had not been elongated) by anion-exchange chromatography (see below). The total elongation was measured by gel electrophoresis as described below. The amount elongated by incorporation of C was calculated by subtracting the amount elongated by T from the total elongation.

Addition of the Next Correct Nucleotide after a Thymine or a Cytosine Base Paired with an O^6-Methylguanine in the Template Strand. DNA duplexes B, C, and D were used to study the rates of the next correct nucleotide after a thymine (duplex B) or a cytosine (duplex C) that has been base paired with O^6-methylguanine in the template strand. Duplex D, which contained a 3′-terminal thymine in the primer strand paired with adenine in the template strand, was included as a control. A solution containing 50 μM dNTP (N = A for duplexes B and C, and N = C for duplex D), 1 μM primer–template, 0.02 μM Klenow fragment, 50 mM Tris·HCl (pH 7.4), and 5 mM $MgCl_2$ was incubated at 30 °C for 15–120 s. The reaction was quenched into denaturing gel loading buffer (0.05% w/v bromophenol blue and 0.05% w/v xylene cyanole in formamide). The amount of primer elongated was measured as described below.

Measurement of Elongation by Gel Electrophoresis, Autoradiography, and Scintillation Counting. After the reaction, the elongated DNA was separated from the parent primer by electrophoresis using 20% polyacrylamide gels containing 7 M urea. The gels were then dried, and the ^{32}P-labeled DNA was located by autoradiography. The amount of radioactivity present in each band was quantitated by cutting the band out and scintillation counting.

Measurement of Elongation Products from Competition Assays. The products of elongation from the competition assays were separated by ion-exchange chromatography and gel electrophoresis. The primer which had been elongated by addition of T was separated from that which had been elongated by C (and from primer which had not been elongated) by anion-exchange chromatography on a Pharmacia Mono Q HR 5-5 column. The flow rate was 0.7 mL/min, and 10 μL of each reaction sample was injected for analysis. The amount of radioactivity present in each fraction (0.7 mL) was quantitated by scintillation counting. The gradient was as follows: 0–2 min, 100% buffer A; 2–5 min, increasing from 0 to 15% buffer B; 5–25 min, increasing from 15 to 35% buffer B [buffer A, 10 mM NaOH, 0.4 M NaCl (pH 12); buffer B, 10 mM NaOH, 0.8 M NaCl (pH 12)].

The total elongation was measured by gel electrophoresis as described above. The amount elongated by incorporation of C was calculated by subtracting the amount elongated by T from the total elongation.

Computer Analysis of Data To Determine Rate Constants. Rate constants for the incorporation of a single nucleotide opposite O^6-methylguanine in the template DNA strand were calculated by mathematical analysis of the results obtained (i.e. the observed extent of elongation as a function of time) to the reaction scheme depicted in Figure 1 using the computer program FACSIMILE (United Kingdom Atomic Energy Authority, Harwell; available from ARC Scientific, 257 Woodstock Road, Oxford OX2 7AE, England), a program for analyzing data which depends on processes that can be described by differential equations. The program was run on an IBM 386 fitted with an Intel 80387 SX math coprocessor.

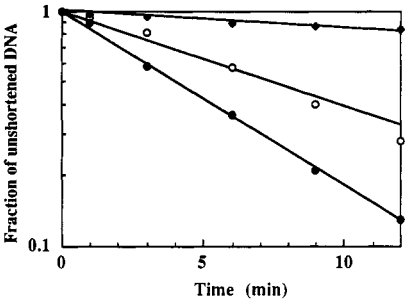

FIGURE 3: 3′ → 5′ exonuclease activity on duplexes B–D using 0.05 μM labeled DNA duplex and 0.1 μM Klenow fragment. In duplexes B (○) and C (●), the 3′-terminal base of the primer was either thymine or cytosine, paired with an O^6-methylguanine in the template strand. The k_{exo} for each DNA duplex was measured as described in the Materials and Methods section (duplex B $k_{exo} = 1.6 \times 10^{-3}$ s^{-1}; duplex C $k_{exo} = 2.8 \times 10^{-3}$ s^{-1}). In duplex D (◆), the 3′ terminal thymine was paired with an adenine ($k_{exo} = 6.5 \times 10^{-4}$ s^{-1}).

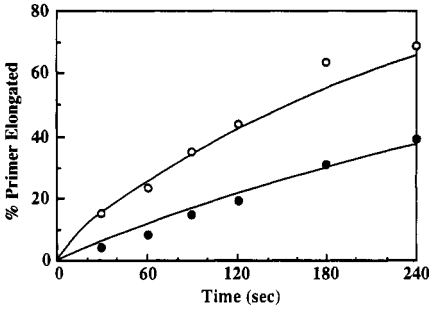

FIGURE 4: Steady-state incorporation of thymine (○) or cytosine (●) opposite O^6-methylguanine in the template strand. The points are the results of incubating DNA duplex A (1 μM) with Klenow fragment (0.1 μM) and 20 μM dTTP or dCTP. The lines are the outcome which would have been predicted from the rate constants in Table 2, which had been calculated from the comparison of the incorporation of the normal and the α-thio nucleotides.

RESULTS

3′→5′ Exonuclease Activity on a Primer with a 3′-Terminal Thymine or Cytosine Base Paired with O^6-Methylguanine in the Template DNA Strand. Figure 3 shows the 3′ → 5′ exonuclease activity of Klenow fragment on a primer with a 3′-terminal thymine or cytosine base paired with O^6-methylguanine in the template DNA strand; a parallel experiment using a duplex containing a 3′-terminal thymine base paired with an adenosine in the template strand was included as a control. The exonuclease rates were calculated from the graphs of log (fraction of unshortened DNA) against time (Figure 3).

Steady-State Incorporation of Thymine or Cytosine opposite Template O^6-Methylguanine in the Template Strand. Figure 4 shows the steady-state incorporation of thymine and cytosine opposite O^6-methylguanine in the template DNA strand. These experiments were carried out with a 10-fold excess of DNA (1 μM) over Klenow fragment (0.1 μM) and 20 μM dNTP. The graph for the incorporation of thymine opposite template O^6-methylguanine does not extrapolate to

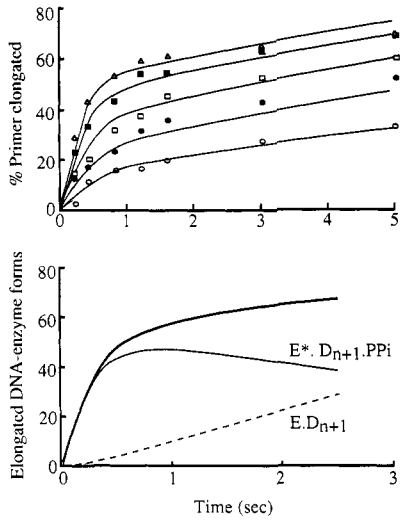

FIGURE 5: Pre-steady-state incorporation of thymine opposite O^6-methylguanine in the template strand using an excess of Klenow fragment over DNA: 0.12 μM Klenow fragment and 0.1 μM duplex A were incubated with 5 (○), 10 (●), 20 (□), 40 (■), and 80 μM (△) dTTP. The points are the experimental results. The lines are the outcome which would have been predicted from the rate constants in Table 2 which had been calculated from the comparison of the incorporation of normal and α-thio nucleotides. The lower figure, using the data for the incorporation of 80 μM dTTP as an example, shows that these progress curves are biphasic because they represent the sum of two component curves: the fast initial rise is primarily a reflection of the accumulation of $E^*{\cdot}D_{n+1}{\cdot}PPi$, while the second apparently steady-state phase reflects the conversion of that into $E{\cdot}D_{n+1}$. There is negligible accumulation of $E{\cdot}D_{n+1}{\cdot}PPi$ because the pyrophosphate dissociates very rapidly. It can be seen from this that the shape of the curve is strongly influenced by the rate of polymerization and by the rate of the second conformational change, and conversely how the internal rate constants can be determined by mathematical analysis of the progress curves.

zero on the vertical axis but intercepts it at approximately 0.05 μM at zero time. This initial rapid polymerization before the steady state is achieved (the pre-steady-state burst) represents polymerization of the DNA to which the enzyme was originally bound. The presence of this pre-steady-state burst shows that the rate of the steady state is limited by a postsynthetic event rather than by the rate of polymerization. This is discussed at greater length below. The points between 30 and 120 s fell onto a straight line with a slope equivalent to 0.029 μmol/(s μmol enzyme). This represents the lower limit for the value of the rate-limiting postsynthetic event. This is of similar magnitude to the dissociation rate of Klenow fragment from a 14/20-mer duplex DNA (0.06 s^{-1}, Kuchta et al., 1987).

In contrast to the case of thymine, there was no evidence for any pre-steady-state burst with cytosine. This indicates that with cytosine the rate of polymerization is the predominant factor limiting the rate of the steady state and that in this case the overall rate [0.016 μmol/(s μmol of enzyme)] is not limited by the rate of some reaction occurring after the actual addition of the nucleotide

Pre-Steady-State Incorporation of Thymine or Cytosine opposite O^6-Methylguanine. The pre-steady-state incorporation (i.e. incorporation on a pre-existing enzyme–DNA complex) of thymine or cytosine opposite O^6-methylguanine in the template strand is shown in Figures 5 and 6. These experiments were performed with 0.1 μM DNA and 0.12 μM Klenow fragment and 5, 10, 20, 40, and 80 μM dNTP. The amount of primer strand elongated was measured at intervals between 200 ms and 16 s. Under similar conditions, the initial rate of incorporation of cytosine opposite O^6-methylguanine

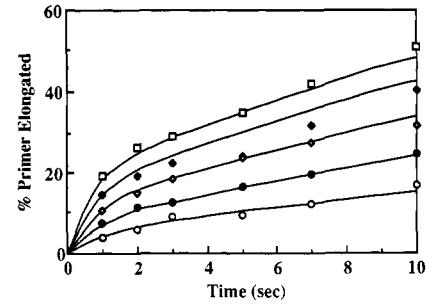

FIGURE 6: Pre-steady-state incorporation of cytosine opposite O^6-methylguanine in the template strand using an excess of Klenow fragment over DNA: 0.12 μM Klenow fragment and 0.1 μM duplex A were incubated with 5 (○), 10 (●), 20 (◇), 40 (◆), and 80 μM (□) dCTP. The points are the experimental results. The lines are the outcome which would have been predicted from the rate constants in Table 2 which have been calculated from comparison of the incorporation of normal and α-thio nucleotides.

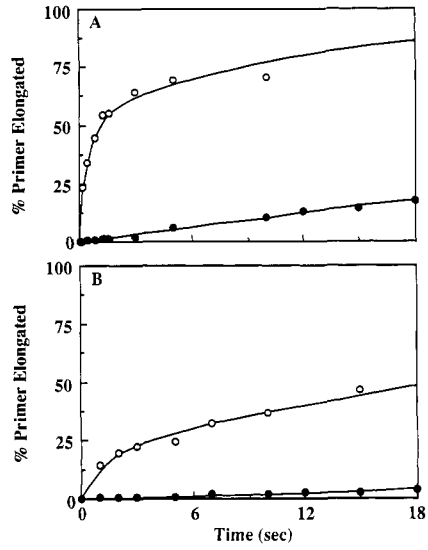

FIGURE 7: Comparison of the incorporation of normal (○) and phosphorothioate nucleotide analogues (●) opposite O^6-methylguanine in the template strand. 0.12 μM Klenow fragment and 0.1 μM duplex A were incubated with 40 μM dTTP or S_p-dTTPαS (A), or 40 μM dCTP or S_p-dCTPαS, (B). The points are the experimental results. The lines for the incorporation of the oxo-dNTPs are the predicted outcome from rate constants in Table 2 and the kinetic scheme in Figure 1. The lines through the data points for the incorporation of the thio-dNTPs were obtained from the assumption that all the rate constants in Table 2, except for k_4 and k_{-4}, are the same for oxo-dNTP and thio-dNTP incorporation. This is discussed in more detail in the text.

in the template strand was roughly 4.7 times slower than that for the incorporation of thymine opposite O^6-methylguanine. Pre-steady-state kinetics of incorporation of the *S*-stereoisomer of the 2′-deoxynucleoside 5′-*O*-(1-thiotriphosphates), (S_p)-dTTPαS or (S_p)-dCTPαS, opposite O^6-methylguanine in the template DNA strand are shown in Figure 7. The rate of incorporation using 40 μM (S_p)-dTTPαS (Figure 7A) was linear with a very shallow gradient (approximately 0.9% elongated per second). This rate was approximately 75 times slower than the initial rate of incorporation using the same concentration of the normal dTTP (approximately 70% elongated per second). Like the case of (S_p)-dTTPαS, the rate of incorporation of 40 μM (S_p)-dCTPαS opposite O^6-methylguanine was also linear over the observation period (18 s) and also approximately 75 times slower than the incorporation of the normal cytosine nucleotide opposite O^6-methylguanine in the template strand. Thus, although thymine and cytosine are incorporated opposite O^6-methylguanine in

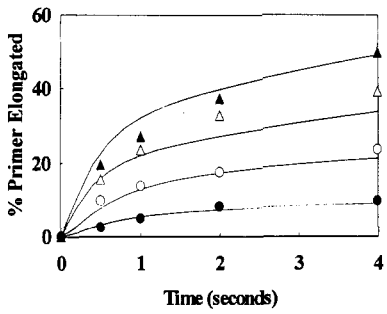

FIGURE 8: Incubation of Klenow fragment and DNA with mixtures of dTTP and dCTP. The points are the experimentally measured incorporation of T and C from two competition assays: incorporation of thymine (▲) and cytosine (●) with 20 μM dTTP + 20 μM dCTP; and incorporation of thymine (△) and cytosine (○) with 20 μM dTTP + 80 μM dCTP. The lines are the outcome predicted from the rate constants in Table 2 which have been calculated from the competition data and the kinetic scheme shown in Figure 1, including a nucleotide-exchange step. The fit to the data points ▲, ●, and ○ was virtually identical if this exchange step was omitted. However, if the exchange step was omitted, the incorporation of T with 20 μM dTTP + 80 μM dCTP (△) was significantly underestimated.

the template strand with different rates, they are affected to the same degree when these normal thymine and cytosine nucleotides are replaced by their respective phosphorothioate nucleotide analogues.

Pre-Steady-State Incorporation of a Mixture of dTTP and dCTP opposite O^6-Methylguanine in the Template Strand. The pre-steady-state incorporation of T and C when the enzyme–DNA complex was incubated with mixtures of dTTP and dCTP (20 μM dTTP; 20 μM dTTP + 20 μM dCTP; and 20 μM dTTP + 80 μM dCTP) is shown in Figure 8.

Calculation of k_{-2}–k_{-5} from Pre-Steady-State Data. In Figures 5–8, the solid lines were generated by using the rate constants shown in Table 2. The rate constants were calculated by the program FACSIMILE on the basis of the reaction scheme shown in Figure 1. Some assumptions were made in order to begin calculations. Second-order rate constants for diffusion-controlled processes (i.e. k_1, k_2, k_{-6}, and k_{-7}), were assumed to be 10^7 M^{-1} s^{-1}. Kuchta et al. (1987) used a value of 1.2×10^7 M^{-1} s^{-1}, and Patel et al. (1991) used a value of 1.1×10^7 M^{-1} s^{-1} for the binding of DNA to Klenow fragment and T7 DNA polymerase, respectively, but Eger and Benkovic (1992) used 1×10^8 M^{-1} s^{-1} for the binding of dNTP to the enzyme–DNA complex. A rate of 0.05 s^{-1} was assumed for the dissociation of the enzyme from the DNA primer–template (k_{-1} and k_7) because Kuchta et al. (1987) reported an equilibrium constant of 5 nM for the binding of a 13/20-mer to Klenow. The rate constant k_6 for the release of pyrophosphate ($E{\cdot}D_1{\cdot}PP_i \rightleftharpoons E{\cdot}D_1 + PP_i$) was assumed to be 1000 s^{-1}. This value was calculated from a reported equilibrium constant of 100 μM for this step (Kuchta et al., 1987); however, later the same laboratory reported that the equilibrium constant may be 230 μM (Dahlberg & Benkovic, 1991).

The remaining rate constants were calculated by nonlinear least square analysis using the computer program FACSIMILE. The data for the incorporation of all five concentrations of nucleoside triphosphates and for the incorporation of the 2′-deoxynucleoside 5′-*O*-(1-thiotriphosphates) were entered as a single data set. The errors were calculated from the natural logarithm of the value for the rate constant; i.e., a log–normal distribution was assumed. Since the rate constants are cross-correlated (i.e., a change in one can be compensated for to some extent by a reciprocal change in another constant), an uncertainty in any constant will induce a systematic uncertainty in every other rate constant. The magnitude of this uncertainty can only be calculated if the correlation between each constant is known. For this reason a correlation matrix between every constant was calculated and used to calculate the correct confidence intervals. The calculated rate constants are given in Table 2. The enzyme and DNA were mixed and allowed to equilibrate before the dNTP and magnesium ions were added to begin the reaction. At the concentrations of enzyme and DNA used (0.12 μM Klenow and 0.1 μM DNA), almost all the DNA was present as enzyme–DNA complex.

Two constraints were used to limit the possible values of the rate constants. First the overall Gibbs free energy change (ΔG) was assumed to be –4 kcal/mol (taken from Patel et al. (1991)), thus fixing the overall equilibrium constant k_{eq}, i.e. the ratio of the forward to the backward rates, as 1000. The justification for the assumed overall free energy change is given in the Discussion section. Second, it was assumed that the thio substitution affected only the forward and backward rates of the bond-formation step, k_4 and k_{-4}, and that all the other rate constants for the incorporation of the phosphorothioate nucleotide analogues ((S_p)-dNTPαS) remained unchanged (Benkovic & Schray, 1973; Eger & Benkovic, 1992). It should be noted that although the literature suggests that the phosphorothioate effect is 100 (Benkovic & Schray, 1973; Mizrahi et al., 1985; Kuchta et al., 1987, 1988), mathematical analysis showed that a value of 150–180 would be needed to explain the observed decrease in the rate of incorporation of (S_p)-dTTPαS and (S_p)-dCTPαS opposite O^6-methylguanine in the template strand if thio substitution affects only k_4 and k_{-4}. Thus, in these calculations, the thio elemental effect was assumed to be 150.

The validity of the rate constants obtained by this mathematical analysis was tested in two ways. First they were used to predict the progress of independently measured steady-state progress curves (Figure 4). There was a close fit between predicted and observed values. Second the K_m was calculated (see appendix) from the calculated rate constants and shown to be in close agreement with the observed K_m (for thymine, observed K_m = 27.6 μM, calculated K_m = 30.7 μM [5% and 95% confidence limits = 27.6 and 34.4 μM]; and for cytosine, observed K_m = 26.4 μM, calculated K_m = 25.5 μM [5% and 95% confidence limits = 21.4 and 35 μM].

Further support was obtained when an independent set of rate constants was calculated from the progress of incorporation of C and T when a mixture of dCTP and dTTP was used (20 μM dTTP + 20 μM dCTP; and 20 μM dTTP + 80 μM dCTP). The results of this experiment (Figure 8) were taken with a similar number of the results from the experiments in which elongation with a single nucleotide had been measured (the results with single nucleotides were not taken in total because that would have weighted the experiment away from the competition), and the combined data set was analyzed mathematically. This latter data set did not contain any data for the incorporation of thio nucleotides and not did not rely on any assumption about the thio effect. It was found that three of the four experimental curves from the competition (i.e. the incorporation of C from 20 μM dTTP plus 20 μM dCTP; and from 20 μM dTTP plus 80 μM dCTP; and the incorporation of T from 20 μM dTTP with 20 μM dCTP) could be closely fitted using the reaction scheme in Figure 1, but the incorporation of T in the competition experiment with 20 μM dTTP with 80 μM dCTP was always significantly underestimated by this reaction scheme. If, however, one allowed an additional step of nucleotide exchange (E·DNA·dTTP + dCTP ⇌ E·DNA·dCTP + dTTP, with

Table 2: Rate and Equilibrium Constants for the Incorporation by Klenow Fragment of Thymine opposite O^6-Methylguanine in the Template DNA Strand[a]

		thymine (5%–95% limits)		cytosine (5%–95% limits)	
reaction	constants	from competition	from thio data	from competition	from thio data
E + D = E·D	k_1[b]	1×10^7	1×10^7	1×10^7	1×10^7
enzyme binds DNA	k_{-1}	0.05	0.05	0.05	0.05
	k_{-1}/k_1[c]	5 nM	5nM	5nM	5nM
E·D + N = E·D·N	k_2[b]	1×10^7	1×10^7	1×10^7	1×10^7
complex binds nucleoside	k_{-2}[d]	1000	1000	1000	1000
triphosphate	k_{-2}/k_2	100 μM	100 μM	100 μM	100 μM
E·D·N = E*·D·N	k_3	24.6 (4.8–126)	59.1 (33–105)	10.6 (1.4–77)	13.1 (3.6–47)
conformational change	k_{-3}	8.4 (1.1–66)	22.2 (11.7–42)	4.6 (0.54–39)	3.82 (0.95–15)
	k_3/k_{-3}	2.9 (0.16–53)	2.67 (2.3–3.1)	2.3 (1.4–3.7)	3.42 (2.7–4.4)
E*·D·N = E*·D_{n+1}·PPi	k_4	3.86 (2.0–7.3)	3.79 (3.4–4.2)	0.73 (0.35–1.5)	0.65 (0.57–0.74)
formation of phosphodiester	k_{-4}	1.93 (0.7–5.6)	1.71 (1.5–1.9)	0.91 (0.24–3.6)	1.35 (1.1–1.6)
bond	k_4/k_{-4}	2.00 (1.2–3.4)	2.21 (1.9–2.5)	0.79 (0.37–1.7)	0.48 (0.4–0.6)
E*·D_{n+1}·PPi = E·D_{n+1}·PPi	k_5	0.35 (0.2–0.6)	0.25 (0.2–0.3)	0.23 (0.09–0.6)	0.23 (0.17–0.31)
relaxation of conformation	k_{-5}	0.0021 (0.0016–0.0027)	0.0015 (0.0013–0.0017)	4×10^{-4} ($2.6–6.8 \times 10^{-4}$)	3.7×10^{-4} ($3.2–4.4 \times 10^{-4}$)
	k_5/k_{-5}	170 ($1.7–1 \times 10^4$)	170 (152–189)	547 ($27–1 \times 10^4$)	610 (473–786)
E·D_{n+1}·PPi = E·D_{n+1} + PPi	k_6[c]	1000	1000	1000	100
release of pyrophosphate	k_{-6}[b]	1×10^7	1×10^7	1×10^7	1×10^7
	k_6/k_{-6}	100 μM	100 μM	100 μM	100 μM
E·D_{n+1} = E + D_{n+1}	k_7[c]	0.05	0.05	0.05	0.05
dissociation of enzyme and	k_{-7}[b]	1×10^7	1×10^7	1×10^7	1×10^7
DNA	k_7/k_{-7}	5 nM	5 nM	5 nM	5 nM
E·D_{n+1} = E·D + NMP	k_{exo}	0.0016		0.0028	
3′ to 5′ exonuclease activity					
Michaelis–Menten constant					
from initial rate	K_m	27.6 μM		26.6 μM	
calculated from rate constants	K_m	33.4 (24.0–46.7)	30.7 (27.6–34.3)	33.4 (24.0–46.7)	25.5 (21.4–30.5)
E·D·dCTP + dTTP = E·D·dTTP	$k_{forward}$	1.9×10^7			
+ dCTP nucleotide exchange	k_{back}	1.0×10^7			

[a] Values determined by mathematical analysis are given with their 5% and 95% confidence limits. [b] Encounter limited rate constants (Kuchta et al., 1987). [c] Taken from Kuchta et al. (1987). [d] The reasons for assuming this value are given in the text.

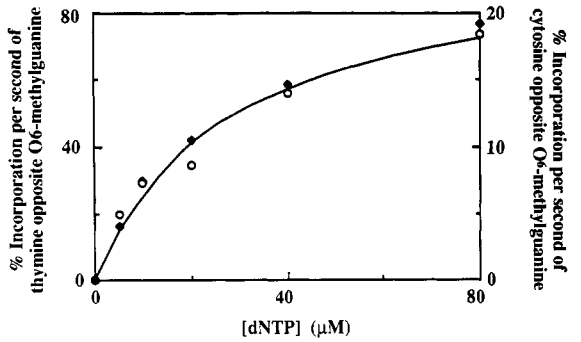

FIGURE 9: Initial rates of incorporation of thymine (○) or cytosine (◆) opposite O^6-methylguanine in the template strand. Klenow fragment (0.12 μM) and DNA duplex A (0.1 μM) were incubated with 5–80 μM dTTP or dCTP. The reaction was stopped after 200 ms for dTTP and 1 s for dCTP. Note that the scales for dTTP and dCTP differ. The line is a Michaelis–Menten fit to these results implying K_m(dTTP) = 27.6 μM and K_m(dCTP) = 26.4 μM.

forward and reverse rate constants of 10^7 and 1.9×10^7 M^{-1} s^{-1}, respectively), then a reasonable fit to the data points from all experimental conditions was obtained (Figure 8). The rate constants calculated from analysis of this competition experiment are given in Table 2. These rate constants are within the confidence limits for those calculated from the previous data set.

Michaelis–Menten Analysis of the Initial Rates of Incorporation of Thymine and Cytosine opposite O^6-Methylguanine in the Template DNA Strand. Figure 9 shows the Michaelis–Menten analysis of the initial rates of incorporation of thymine and cytosine opposite O^6-methylguanine in the template DNA strand. Note that the scale for the percent incorporation of thymine (0–80%) is different from that for the percent incorporation of cytosine (0–20%). The points are initial rates calculated from the percentage of primer elongated in the first 200 ms (thymine) or first second (cytosine). The line was generated by performing a Michaelis–Menten analysis using Multifit 1.5 (Day Computing, P.O. Box 327, Milton, Cambridge CB4 4WL, England). The values of K_m for the incorporation of thymine and cytosine opposite O^6-methylguanine in the template DNA strand are 27.6 and 26.4 μM, respectively. Although the values of K_m for the incorporation of thymine and cytosine opposite O^6-methylguanine are very similar, the values of V_{max} differ by about 4-fold: 0.97 and 0.25 mol elongated/(s mol of enzyme) for thymine and cytosine, respectively.

Addition of the Next Correct Nucleotide after a Thymine or a Cytosine Base Paired with O^6-Methylguanine in the Template Strand. Figure 10 shows the rates of adding the next correct nucleotide after a T:O^6-MeG, a C:O^6-MeG, and a T:A base pair. The steady-state rate of addition after the T of a T:O^6-MeG base pair is very similar to that of addition after a normal T:A base pair, whereas addition after the C of a C:O^6-MeG base pair is considerably slower.

DISCUSSION

We have carried out steady-state (Figure 4) and pre-steady-state (Figures 5–8) studies on the incorporation of thymine and cytosine opposite O^6-methylguanine in the template DNA strand. The results obtained were analyzed mathematically to determine the rate constants in the reaction scheme shown in Figure 1 and thus to show how *E. coli* Klenow fragment chooses to incorporate thymine in greater amounts than

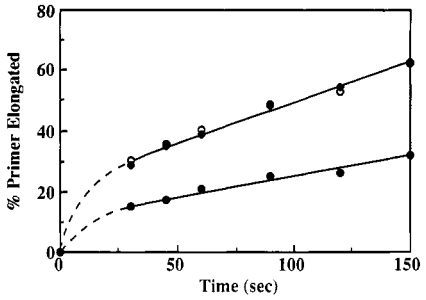

FIGURE 10: Addition of a correct nucleotide following the thymine in an O^6-MeG:T pair (○) the cytosine in an O^6-MeG:C pair (●), or the thymine in an A:T (◆) pair, which was included as control. Klenow fragment (20 nM) was incubated with 1 μM DNA duplex B, C, or D and either 50 μM dATP (duplexes B or C) or 50 μM dCTP (duplex D). Since the steady-state addition of a single nucleotide after a normal base pair is limited by the rate of dissociation of the enzyme from the elongated DNA, the similarity between the rate of incorporation after the O^6-MeG:T and the T:A pair does not imply that the rate of the polymerization step is the same in both cases.

cytosine opposite the promutagenic base O^6-methylguanine in the template DNA strand.

The steady-state incorporation of thymine or cytosine opposite O^6-methylguanine in the template DNA strand, shown in Figure 4, shows a pre-steady-state burst of incorporation of thymine but not of cytosine. Under steady-state conditions almost all the enzyme molecules are bound to DNA (k_d = 5 nM; Kuchta et al., 1987). The elongation during the pre-steady-state burst is largely that of the DNA to which the enzyme is initially bound. Thus the occurrence of this pre-steady-state burst indicates that the steady-state incorporation of thymine is limited predominantly by a postsynthetic event such as the dissociation of the enzyme from the DNA and its binding to another substrate DNA duplex, rather than being limited by the rate of incorporation itself. With cytosine however, there is no appreciable pre-steady-state burst, so the steady-state rate of incorporation is limited predominantly by the rate of incorporation itself.

The incorporation of a single nucleotide by Klenow fragment or T7 DNA polymerase involves five kinetically discernable steps (Figure 1, steps 2–6) (Kuchta et al., 1987, 1988; Patel et al., 1991; Wong et al., 1991; Dahlberg & Benkovic, 1991; Eger & Benkovic, 1992). One needs to ask how the ten rate constants differ so that thymine is preferentially incorporated. To answer this question one needs to carry out pre-steady-state kinetic studies; i.e., start the reaction with all the DNA present as an enzyme–DNA complex and follow one catalytic cycle. The results are shown in Figures 5 and 6. The initial rate of incorporation of thymine and of cytosine, i.e. that in the first 200 ms (T) or 1 s (C), followed by Michaelis–Menten kinetics. Figure 8 shows that although the actual rates of elongation are different, thymine and cytosine have similar K_m values (27.6 and 26.4 μM, respectively), and these K_m values are similar to the values of 8.3–21 μM reported for misincorporations by Klenow fragment (Kuchta et al., 1988).

The pre-steady-state progress curves (Figures 5 and 6) can be regarded as the integration of the differential equations implied by Figure 1. The objective of the analysis of the data is to assign values to the rate constants in Figure 1. This was carried out by using the FACSIMILE program (Chance & Curtis, 1970; Curtis & Chance, 1972; Chance et al., 1977; Curtis & Sweetenham, 1988). All the experimental data shown in Figure 5, or Figure 6, was entered as a single array showing the elongation of the primer at different times with each concentration of dNTP or (S_p)-dNTPαS. The reaction scheme (Figure 1) was also entered. It was found that it was impossible to omit any step in the kinetic scheme and still get a reasonable fit to the data, thus confirming that the reaction scheme in figure 1 is the minimum required. The rate constants that gave the least residual sum of squares fit to the complete data set were calculated. The concentration of each intermediate at various times as well as the flux (mol/(L s)) through each step was calculated. The adequacy of the fit was assessed in several ways. The total residual sum of squares, i.e. the fit of all the data points to their respective curves, was compared with the expected range of the residual sum of squares calculated from the degrees of freedom and the estimated standard deviation of the data points. The residual sum of squares fit to each individual curve, in this case the curve corresponding to each dNTP concentration, was also calculated. A calculation showing whether the residuals to each curve were as likely to be positive as negative and other calculations which also detect systematic errors were made. The ratio of the forward and the backward rate constants was calculated to allow the free energy change for each step to be estimated. The 5% and 95% confidence limits to the natural log of each rate constant were calculated; i.e., a log–normal distribution was assumed. Because to some extent it is possible to get an equally good fit by reciprocally changing two rate constants in the scheme—e.g. compensating an increase in a forward rate constant with an increase in a backward rate constant or compensating a decrease in the forward rate to one step by increasing the forward rate to the following step—an error in any rate constant induces a systematic error in every other constant, the magnitude of which depends on the correlation between the constants. The errors shown in Table 2 take account of this. The overall kinetic solution was constrained to the thermodynamics of the process. Kuchta et al. (1988) measured the overall equilibrium constant for the formation of an A:A mismatch by Klenow as 2900 ± 1000, implying ΔG = –4.7 kcal/mol. Patel et al. (1991) calculated ΔG for the incorporation of dTMP into DNA by T7 DNA polymerase as –3.97 kcal/mol, under conditions where [DNA] = 20 nM, [dTTP] = 100 μM, and [PP_i] = 2 mM. We constrained our solution to a ΔG of –4 kcal/mol, i.e. an overall equilibrium constant of 1000. Changing the value chosen for the equilibrium constant did not make a significant change to the calculated value of any constant except k_{-5} (see below).

In analyzing the data in Figures 5 and 7a, or in 6 and 7b, the second constraint used was to compare the rates of incorporation of regular dNTP and their phosphorothioate analogues (S_p)-dNTPαS into DNA. Because sulfur is less electronegative than oxygen, incorporation of (S_p)-dNTPαS into DNA is slower. The thio substitution alters the rate constants for the chemistry step (i.e. k_4 and k_{-4}) and does not materially affect the binding of the dNTP to the Klenow–DNA complex or the rate of the first conformational change (Benkovic & Schray, 1973; Eger & Benkovic, 1992). The exact magnitude of this thio effect on rate constants is not known, but until 1991 it was assumed that the formation of a phosphothiodiester bond by DNA polymerase, and its hydrolysis, using (S_p)-dNTPαS was approximately 100 times slower than the formation or hydrolysis of the normal phosphodiester bond (Mizrahi et al., 1985; Kuchta et al., 1988; Patel et al., 1991). If during polymerization the formation of a phosphodiester bond between the 3′-OH group of the deoxyribose sugar at the primer terminus and the α-phosphate of the incoming dNTP is rate-limiting, then the rate of polymerization using the phosphorothioate analogue of the regular deoxynucleotide triphosphate, (S_p)-dNTPαS, should

decrease by approximately 100-fold. In normal nucleotide incorporation, the phosphorothioate nucleotide was incorporated only 3–7-fold slower than the normal (Kuchta et al., 1987; Patel et al., 1991), which was taken as evidence that the formation of the phosphodiester bond is not rate-limiting. In the formation of mismatches, the ratio is higher but still much smaller than 100. For example, for the formation of A:A mismatches by Klenow, the ratio of the rate of incorporation of oxo-dNTP/thio-dNTP is about 65 (Kuchta et al., 1988); with an exo mutant of Klenow, it is 40 or 20, depending on the DNA template (Eger et al., 1991) (later, the smaller of these two ratios was redetermined as 12.5 (Eger & Benkovic, 1992), and with T7 DNA polymerase, the ratios for the formation of A:A, C:A, and G:A mismatches by incorporating adenine, cytosine, or guanine opposite adenine in the template DNA strand are 19, 17, and 37, respectively (Wong et al., 1991).

The rates of incorporation of the corresponding (S_p)-dTTPαS and of (S_p)-dCTPαS (both 20 μM) opposite template O^6-methylguanine were about 75 times slower than those for the incorporation of the regular nucleotides (Figure 7). This indicates that the formation of the phosphodiester bond is the rate-limiting step. The objective of the mathematical analysis was to fit a combined data set of incorporation of both regular nucleotides and their phosphorothioate analogues by a single set of rate constants differing only by the fact that k_4 and k_{-4} for the phosphorothioate nucleotide analgoues are slower than k_4 and k_{-4} for the regular nucleotides. This constraint fixes the values of k_4 and k_{-4} to within very close limits. Mathematical analysis showed that if the underlying assumption, that α-thio substitution affects only the rates k_4 and k_{-4}, is correct, then these must be decreased around 150–180-fold to explain the observed thio effect on the rate of incorporation. Thus, the results of the incorporation of both normal nucleotides and their phosphorothioate analogues (e.g. the data in Figure 7) were analyzed as a single set of data, linked by the relationship that $k_4(\text{oxo})/k_4(\text{thio}) = k_{-4}(\text{oxo})/k_{-4}(\text{thio}) = 150$.

It proved impossible to determine k_{-2} within reasonable limits from this set of data because the initial product of the reaction (E·D·N) has a very low maximum concentration and any change in k_{-2} could be compensated for by changes in k_3 or k_{-3}. The literature suggests a value of 1000 s^{-1} (Kuchta et al., 1988). Trial calculations showed that the data could not be fit if k_{-2} was fixed at significantly less than 500 or more than 1500 s^{-1}; i.e., k_D must be between 50 and 150 μM. Varying k_{-2} from 500 to 1000 or 1500 s^{-1} produced a compensating change in k_3 and k_{-3}, but the ratio k_3/k_{-3} remained the same, and to satisfy the constraint on k_{eq}, there was a change in k_{-5}. Sensitivity analysis (Vajda et al., 1985) showed that it was possible to change the value of k_{-5} in this way because the concentration of none of the enzyme-linked forms depend on this value. Following these trials a value of 1000 s^{-1} for k_{-2} was assumed (i.e. k_D = 100 μM), which allowed the internal rate constants shown in Table 2 to be calculated. The only significant difference between the rate constants for incorporation of thymine and of cytosine is a 5-fold difference in the rate of the formation of the phosphodiester link.

The progress curves for the incorporation of either C or T are biphasic with a rapid initial phase followed by a slower apparently steady-state phase (Figures 6 and 7). Mathematical deconvolution of each curve showed (Figure 6) that these progress curves are biphasic because they represent the sum of the accumulation of E*·D_{n+1}·ppi and E·D_{n+1}. The rapid initial phase is the accumulation of the former, with the slower second phase reflecting the passage of the former through the conformational step. Because k_6 is much greater than k_5, there is negligible accumulation of E·D_{n+1}·ppi. This analysis shows how the shapes of the curves are a reflection of the internal rate constants and thus how those rate constants can be obtained from the mathematical analysis. It also gives direct mathematical evidence for the existence of the second conformational change.

Two checks were made to establish whether the constants calculated from analysis of the data in Figures 6 and 7 were correct. First the K_m (see Appendix) was calculated from the constants and compared with the approximate K_m obtained from the Michaelis–Menten analysis of initial rates (Figure 9). The calculated K_m values for thymine (30.7 μM, with 5% and 95% confidence limits of 27.6 and 34.4 μM) and for cytosine (25.5 μM, with 5% and 95% confidence limits of 21.4 and 35 μM) are statistically indistinguishable from the values obtained by Michaelis–Menten analysis of the initial rates (27.6 and 26.4 μM for thymine and cytosine, respectively). The second check was to predict the course of steady-state experiments from the calculated rate constants and compare the prediction with the actual results of steady-state experiments. This is shown in Figure 4, where it can be seen that the actual and predicted results are very similar although not exactly the same. The reasonable correspondence between the actual and the predicted K_m values and the actual and predicted steady-state incorporation leads to the conclusion that the calculated rate constants cannot be substantially in error.

However, when this was presented for publication, the reviewers brought to our attention the paper by Hershlag et al. (1991), which proposed that the elemental affect of thio substitution would be between 4 and 11, and suggested that our conclusions might therefore be in error. To settle this point, competition experiments were done in which the enzyme–DNA complex was incubated with mixtures of different concentrations of dCTP and dTTP and the time course of incorporation of cytosine and thymine measured. The results of this experiment (Figure 8) were taken with a similar number of the results from the experiments in which elongation with a single nucleotide had been measured (the results with single nucleotides were not taken in total because that would have weighted the experiment away from the competition). This combined data set was analyzed mathematically. It was found that three of the four experimental curves (i.e. the incorporation of C from 20 μM dTTP plus 20 μM dCTP; and from 20 μM dTTP plus 80 μM dCTP; and the incorporation of T from 20 μM dTTP with 20 μM dCTP) could be closely fitted using the reaction scheme shown in Figure 1, but the incorporation of T in the competition experiment with 20 μM dTTP with 80 μM dCTP was always significantly underestimated by a mathematical fit to this scheme. If, however, one allowed an additional step of nucleotide exchange (E·DNA·dTTP + dCTP $\rightleftharpoons$ E·DNA·dCTP + dTTP, with forward and reverse rate constants of 10^7 and 1.9×10^7 M^{-1} s^{-1}, respectively), then a reasonable fit to the data points from all experimental conditions was obtained (Figure 8). A nucleotide exchange of this kind could make a significant contribution to fidelity, and for this reason experiments to confirm whether it actually exists are underway. Two constraints were put on the solution: as before, the total Gibbs free energy change was assumed to be –4 kcal/mol; and as the measured K_m for the incorporation of thymine (27.6 μM) was very similar to that for the incorporation of cytosine (26.4 μM) (Figure 9), these K_m values were assumed to be equal. The rate constants obtained from this analysis

Table 3: Approximate Gibbs Free Energy Changes (ΔG) in kcal/mol for the Incorporation by Klenow Fragment of Different Nucleotides opposite O^6-Methylguanine, Compared with ΔG Calculated from Previously Published Rate Constants for the Incorporation by Klenow Fragment or T7 DNA Polymerase

reaction	T opp O^6-MeG[b] (Klenow)	C opp O^6-MeG[b] (Klenow)	T opp A[c] (T7 DNA polymerase)	T opp A[d] (Klenow)	A opp A[e] (Klenow)
E·D·N = E*·D·N	−0.64	−0.5	−0.64	−1.67	−1.2
E*·D·N = E*·D_{n+1}·PPi	−0.43	+0.14	+0.40	−0.82	−1.3
E*·D_{n+1}·PPi = E·D_{n+1}·PPi	−3.03	−3.73	−2.48	0.00	−2.1

[a] These values are in kcal/mol calculated from $\Delta G = -RT\ln K_{eq}$, where K_{eq} is the equilibrium constant for each reaction. E is enzyme; E*, enzyme after the conformational change; D, DNA; D_{n+1}, DNA after elongation: N, dNTP; PPi, pyrophosphate. [b] See Table 2. [c] Calculated from rate constants taken from Patel et al. (1991). [d] From Dahlberg and Benkovic (1991). [e] From Eger and Benkovic (1992).

are given in Table 3. The same table gives the rate constants obtained, as described above, from comparison of the incorporation of normal and thionucleotide triphosphates. It can be seen from the table that the maximum likelihood values of the rate constants derived from the competition with normal nucleotides are indistinguishable from those obtained making the assumption about the incorporation of thionucleotides. The analysis of data from the competition experiments allowed the value of k_{-2} for the incorporation of C to be estimated as 880 s^{-1} (617–1250). Substitution of this value for the assumed value of 1000 s^{-1} made no appreciable difference to the other calculated values. It was still impossible to calculate k_{-2} for the incorporation of T, and therefore a value of 1000 s^{-1} was assumed.

The paper by Hershlag et al. (1991), which suggested that the elemental (thio) effect on the rate of formation and hydrolysis of phosphodiesters is to decrease these constants between 4- and 11-fold, has thrown doubt on previous published rate constants for DNA synthesis which were obtained assuming a thio effect of 100–160 (reviewed by Johnson (1993)). Our results may be fortuitous, but they suggest that the previous assumption of the scale of the elemental effect did not lead to the calculation of erroneous rate constants. One must also question whether the Hershlag et al. (1991) analysis is applicable to DNA synthesis. Eger and Benkovic (1992) have shown that thionucleotides bind to the enzyme–DNA complex as well as do normal nucleotides and that the rate of the first conformational change is also the same. It is difficult to reconcile the observation that the rate of incorporation of thionucleotides into mismatches by Klenow is up to 65-fold (Kuchta et al., 1988), 20- or 40-fold (Eger et al., 1991), and 12.5-fold (Eger & Bencovic, 1992) less than the rate of incorporation of normal nucleotides, if the elemental effect on the rate of polymerization is only 4–11-fold. It must be remembered that the measurements of incorporation are made after a finite time and thus are the integrated flux through the polymerization step over that time period. The magnitude of the decrease in the flux is less than the magnitude of the change in the rate constant for the polymerization step because any decrease in rate constant is partly compensated for by an increase in the concentration of the enzyme form immediately before the affected step and a decrease in the concentration of the form immediately after the affected step. In the present case if one assumes a thio elemental effect of 180, the ratio of the flux through the polymerization step (flux oxo-dNTP/flux thio-dNTP) falls to only 37 within 0.5 s of the start of the reaction. Thus even the lowest ratio of 12.5 recorded by Eger and Benkovic (1992) is inconsistent with a simple comparison with the results of Hershlag et al. (1991).

After it was realized that O^6-methylguanine does not form a more stable base pair with thymine than with cytosine (Gaffney & Jones, 1989), the discussion of the misincorporation of thymine opposite O^6-methylguanine focused on two possibilities: (1) discrimination through K_m possibly because of the structural similarities between O^6-methylguanine and adenine (an analogous situation would be the recognition of O^6-methylguanine by adenosine deaminase (Pegg & Swann, 1979)); (2) that the discrimination occurred because the O^6-methylG:T base pair retains the Watson–Crick configuration (where N1 of the purine is juxtaposed to N3 of the pyrimidine) while the O^6-methylG:C base pair is a wobble pair (Patel et al., 1986a,b; Goswami et al., 1993; reviewed by Swann (1990)).

The results reported now showing that the discrimination occurs at the formation of the phosphodiester link support the view that the Watson–Crick conformation of the O^6-methylG:T base pair is the important factor in ensuring the incorporation of thymine opposite O^6-methylguanine. The reason for this is probably the distortion of the phosphodiester link which occurs on the formation of the wobble O^6-methylG:C base pair. The presence of an O^6-alkylG:C base pair perturbs the ^{31}P NMR spectrum. The phosphorus resonances of dodecamer DNA duplexes containing either O^6-ethylG:T or O^6-ethylG:C base pairs have been assigned (Kalnik et al., 1988a,b). This assignment showed that the greatest change from the spectrum of the control dodecamer with a G:C base pair was in the chemical shift of the phosphodiester link 5′ to the cytosine in the O^6-ethylG:C base pair (moved 0.59 ppm upfield) and in that of the phosphodiester link 3′ to the cytosine (moved 0.5 ppm downfield). The possible relation between such chemical shifts and the conformation of the phosphodiester has been discussed by Gorenstein et al. (1988). It seems reasonable to ascribe the slow incorporation of cytosine opposite O^6-methylguanine to the stereochemical problems of aligning the 3′-OH of the primer strand with the α-phosphorus of the nucleoside triphosphate.

If a distortion of the phosphodiester backbone impairs the incorporation of cytosine opposite O^6-methylguanine because it presents problems in aligning the 3′-OH of the primer with the α-phosphorus of the incoming dCTP, one might expect the addition of a correctly paired nucleotide after a cytosine in a C:O^6-MeG base pair to be slower than the corresponding addition after thymine in a O^6-MeG:T base pair. Figure 10 shows that in steady-state polymerization experiments, addition of the nucleotide after the cytosine in an O^6-MeG:C base pair is slower than that after a thymine in a T:O^6-MeG base pair.

Table 3 shows the approximate Gibbs free energy changes for the incorporation of thymine and cytosine opposite O^6-methylguanine in the template DNA strand and compares them with the free energy changes for the incorporation of normal nucleotide triphosphates by Klenow fragment (Dahlberg & Benkovic, 1991) and T7 DNA polymerase (Patel et al., 1991). In the incorporation of thymine or cytosine opposite O^6-methylguanine in the template strand, the major part of the overall Gibbs free energy change for the process comes from the relaxation step (Figure 1, step 5) where the enzyme in the E*·D_{+1}·PP_i complex changes from an 'energized' state into a 'relaxed' state, after the phosphodiester bond has formed. The significance of this is that all the steps before this are freely reversible, but once this enzyme relaxation step has occurred, the incorporation is committed and will be reversed only by action of 3′ → 5′ exonuclease or by mismatch repair.

In the formation of an A:A mismatch by Klenow fragment, the greatest part of the energy change is also in the conformational change after the polymerization (Eger & Benkovic, 1992), but for correct incorporation this step is isoenergetic, and the greatest part of the energy is in the conformational change prior to polymerization (Dahlberg & Benkovic, 1991). One interesting aspect of the energetic profile of incorporation opposite O^6-methylguanine is that the incorporation of cytosine is endothermic (ΔG = +0.14 kcal/mol). Patel et al. (1991) suggested that with T7 DNA polymerase this step is also endothermic (ΔG = +0.40 kcal/mol) for the incorporation of thymine opposite adenine.

The overall conclusion from this, and previous studies by others, is that the DNA polymerase has evolved to catalyze the formation of phosphodiesters only when the 3′-OH of the primer strand and the α-phosphorus of the incoming dNTP are in the alignment found in Watson–Crick pairs. Any deviation from this will have a very marked effect on the rate of synthesis. Because the greatest energy change occurs after the formation of the phosphodiester bond, the reverse rates of the early steps are relatively fast, allowing a mismatched base to be replaced without the need for the 3′ to 5′ exonuclease.

ACKNOWLEDGMENT

We are grateful to Dr. Yao-Zhong Xu for his assistance in the synthesis of oligonucleotides containing O^6-methylguanine and Mr. D. Sargent for making the rapid quench apparatus.

APPENDIX

Calculation of K_m and V_{max} Using the Internal Rate Constants. For the reactions

$$\text{E·D} + \text{dNTP} \underset{k_{-2}}{\overset{k_2}{\rightleftharpoons}} \text{E·D·N} \underset{k_{-3}}{\overset{k_3}{\rightleftharpoons}} \text{E*·D·N} \underset{k_{-4}}{\overset{k_4}{\rightleftharpoons}} \text{E*·D}_1\text{·PP}_i$$

the reaction velocities, i.e. the net flux of each reaction, are

$$V_1 = k_2[\text{dNTP}][\text{E·D}] - k_{-2}[\text{E·D·N}] \quad (1)$$

$$V_2 = k_3[\text{E·D·N}] - k_{-3}[\text{E*·D·N}] \quad (2)$$

$$V_3 = k_4[\text{E*·D·N}] - k_{-4}[\text{E*·D}_1\text{·PP}_i] \quad (3)$$

V_3 is the greatest when $[\text{E*·D}_1\text{·PP}_i] = 0$. Thus,

$$V_3 = k_4[\text{E*·D·N}]$$

$$[\text{E*·D·N}] = V_3/k_4 \quad (4)$$

Substituting (4) into (2),

$$V_2 = k_3[\text{E·D·N}] - V_3\frac{k_{-3}}{k_4}$$

$$[\text{E·D·N}] = V_2\frac{k_{-3}}{k_3k_4} \quad (5)$$

Substituting (5) into (1),

$$[\text{E·D}] = \frac{V_1}{[\text{dNTP}]k_2} + \frac{V_2k_{-2}}{[\text{dNTP}]k_2k_3} + \frac{V_3k_{-2}k_{-3}}{[\text{dNTP}]k_2k_3k_4} \quad (6)$$

If the total enzyme concentration is $[E_0]$,

$$[\text{E·D}] + [\text{E·D·N}] + [\text{E*·D·N}] \quad (7)$$

V_{max} is the maximum steady-state velocity. As [dNTP] → ∞, [E·D] → 0 and $V_2 = V_3 = V_{max}$. Therefore, at V_{max}, $[E_0]$ + [E*·D·N], and substituting (4) and (5) into this

$$[E_0] - \left(\frac{V_2}{k_3} + \frac{V_3k_{-3}}{k_3k_4}\right) + \left(\frac{V_3}{k_4}\right)$$

$$[E_0] = V_{max}\left(\frac{1}{k_3} + \frac{k_{-3}}{k_3k_4} + \frac{1}{k_4}\right)$$

$$[E_0] = V_{max}\left(\frac{k_4 + k_{-3} + k_3}{k_3k_4}\right)$$

$V_{max} = K_{cat}[E_0]$, thus

$$K_{cat} = \frac{k_3k_4}{k_4 + k_{-3} + k_3} \quad (8)$$

Equation 7 becomes

$$\frac{V_{max}}{K_{cat}} = \left(\frac{V_1}{[\text{dNTP}]k_2} + \frac{V_2k_{-2}}{[\text{dNTP}]k_2k_3} + \frac{V_3k_{-2}k_{-3}}{[\text{dNTP}]k_2k_3k_4}\right) + \left(\frac{V_2}{k_3} + \frac{V_3k_{-3}}{k_3k_4}\right) + \left(\frac{V_3}{k_4}\right)$$

For [dNTP] = K_m, the reaction rate is $V_{max}/2$, so

$$\frac{V_{max}}{K_{cat}} = \frac{V_{max}}{2K_m}\left(\frac{1}{k_2} + \frac{k_{-2}}{k_2k_3} + \frac{k_{-2}k_{-3}}{k_2k_3k_4}\right) + \frac{V_{max}}{2}\left(\frac{1}{k_3} + \frac{k_{-3}}{k_3k_4} + \frac{1}{k_4}\right)$$

$$\frac{V_{max}}{K_{cat}} = \frac{V_{max}}{2K_m}\left(\frac{k_3k_4 + k_{-2}k_4 + k_{-2}k_{-3}}{k_2k_3k_4}\right) + \frac{V_{max}}{2}\left(\frac{k_4 + k_{-3} + k_3}{k_3k_4}\right)$$

If we put

$$\alpha = \frac{k_3k_4 + k_{-2}k_4 + k_{-2}k_{-3}}{k_2k_3k_4}$$

then

$$\frac{V_{max}}{K_{cat}} = \frac{\alpha V_{max}}{2K_m} + \frac{V_{max}}{2K_{cat}}$$

Multiply both sides of the equation by $2K_{cat}/V_{max}$; the equation becomes

$$2 = \frac{\alpha K_{cat}}{K_m} + 1$$

$$K_m = \alpha K_{cat} \quad (9)$$

REFERENCES

Beese, L. S., & Steitz, T. A. (1991) *EMBO J. 10*, 25–33.
Beese, L. S.; Derbyshire, V., & Steitz, T. A. (1993) *Science 260*, 352–355.
Benkovic, S. J., & Schray, K. J. (1973) in *The Enzymes* (Boyer, P. D., Ed.) pp 201–238, Academic Press: New York.
Bishop, R. E., & Moschel, R. C. (1991) *Chem. Res. Toxicol. 4*, 647–654.
Boosalis, M. S., Petruska, J., & Goodman, M. F. (1987) *J. Biol. Chem. 262*, 14689–14696.
Boosalis, M. S., Mosbaugh, D. W., Hamatake, R., Sugino, A., Kunkel, T. A., & Goodman, M. F. (1989) *J. Biol. Chem. 264*, 11360–11366.

Carroll, S. S., & Benkovic, S. J. (1990) *Chem. Rev. 90*, 1291–1307.
Chance, E. M., & Curtis, A. R. (1970) *FEBS Letts. 7*, 47–50.
Chance, E. M., Curtis, A. R., Jones, I. P., & Kirby, C. R. (1977) Report A.E.R.E. R 8775, Atomic Energy Research Establishment, Harwell, Berkshire, England.
Curtis, A. R. & Chance, E. M. (1972) in *Eighth FEBS Meeting: Analysis and Simulation of Biochemical Systems*, North-Holland/American Elsevier, Amsterdam, The Netherlands.
Curtis, A. R., & Sweetenham, W. P. (1988) Report A.E.R.E. R 12805, United Kingdom Atomic Energy Authority, Harwell, Berkshire, England.
Dahlberg, M. E., & Benkovic, S. J. (1991) *Biochemistry 30*, 4835–4843.
Dosanjh, M. K., Galeros, G., Goodman, M. F., & Singer, B. (1991) *Biochemistry 30*, 11595–11599.
Dosanjh, M. K., Loechler, E. L., & Singer, B. (1993) *Proc. Natl. Acad. Sci. U.S.A. 90*, 3983–3987.
Echols, H., & Goodman, M. F. (1991) *Annu. Rev. Biochem. 60*, 477–511.
Eger, B. T., & Benkovic, S. J. (1992) *Biochemistry 31*, 9227–9236.
Eger, B. T., Kuchta, R. D., Carroll, S. S., Benkovic, P. A., Dahlberg, M. E., Joyce, C. M., & Benkovic, S. J. (1991) *Biochemistry 30*, 1441–1448.
El-Diery, W. S., So, A. G., & Downey, K. M. (1988) *Biochemistry 27*, 546–553.
Englisch, U., Gauss, D., Freist, W., Englisch, S., Sterbach, H., & von der Haar, F. (1985) *Angew. Chem., Int. Ed. Engl. 24*, 1015–1025.
Eritja, R., Horowitz, D. M., Walker, P. A., Zichler-Martin, J. P., Boosalis, M. S., Goodman, M. F., Itakuru, K., & Kaplan, B. E. (1986) *Nucleic Acids Res. 14*, 8135–8153.
Fersht, A. (1985) in *Enzyme structure and mechanism*, W. H. Freeman and Co., New York.
Gaffney, B. L., & Jones, R. A. (1989) *Biochemistry 28*, 5881–5889.
Georgiadis, P., Smith, C. A., & Swann, P. F. (1991) *Cancer Res. 51*, 5843–5850.
Ginell, S. L., Kuzmich, S., Jones, R. A., & Berman, H. M. (1990) *Biochemistry 29*, 10461–10465.
Gorenstein, D. G., Schroeder, S. A., Fu, J. M., Metz, J. T., Roongta, V., and Jones C. R. (1988) *Biochemistry 27*, 7223–7237.
Goswami, B., Gaffney, B. L., & Jones R. A. (1993) *J. Am. Chem. Soc. 115*, 3832–3833.
Graves, R. L., Li, B. F., & Swann, P. F. (1989) *Carcinogenesis 10*, 661–666.
Johnson, K. A. (1993) *Annu. Rev. Biochem. 62*, 685–713.
Kalnik, M. W., Li. B. F. L, Swann, P. F., & Patel, D. J. (1989a) *Biochemistry 28*, 6170–6181.
Kalnik, M. W., Li, B. F. L., Swann, P. F., & Patel, D. J. (1989b) *Biochemistry 28*, 6182–6192.
Kuchta, R. D., Mizrahi, V., Benkovic, P. A., *Johnson*, K. A., & Benkovic, S. J. (1987) *Biochemistry 26*, 8410–8417.
Kuchta, R. D., Benkovic, P., & Benkovic, S. J. (1988) *Biochemistry 27*, 6716–6725.
Kumar, R., Sukumur, S., & Barbacid, M. (1990) *Science 248*, 1101–1104.
Kunkel, T. A. (1992) *J. Biol. Chem. 267*, 15789–15794.
Lawley, P. D., Orr, D. J., Shah, S. A., Farmer, P. B., & Jarman, M. (1973) *Biochem. J. 135*, 193–201.
Leonard, G. A., Thomson, J., Wayson, W. P, & Brown, T. (1990) *Proc. Natl. Acad. Sci. U.S.A. 87*, 9573–9576.
Loeb, L. A., & Reyland, M. E. (1987) in *Nucleic Acids and Molecular Biology* (Eckstein, F., & Lilley, D. M. J., Eds.) pp 157–173, Springer, Berlin.
Loveless, A. (1969) *Nature 223*, 206–207.
Mhaskar, D. N., & Goodman, M. F. (1984) *J. Biol. Chem. 259*, 11713–11717.
Mizrahi, V., Henrie, R. N., Marlier, J. F., Johnson, K. A., & Benkovic, S. J. (1985) *Biochemistry 24*, 4010–4018.
Ollis, D. L, Brick, P., Hamlin, R., Xuong, N. G., & Steitz, T. A. (1985) *Nature 313*, 762–766.
Patel, D. J., Shapiro, L., Kozlowski, S. A., Gaffney, B. L., & Jones, R. A. (1986a) *Biochemistry 25*, 1027–1036.
Patel, D. J., Shapiro, L., Kozlowski, S. A., Gaffney, B. L., & Jones, R. A. (1986b) *Biochemistry 25*, 1036–1042.
Patel, S. S.; Wong, I., & Johnson, K. A. (1991) *Biochemistry 30*, 511–525.
Pegg, A. E., and Swann, P. F. (1979) *Biochim. Biophys. Acta 565*, 241–252.
Petruska, J., Goodman, M. F., Boosalis, M. S., Sowers, L. C., Cheong, C., & Tinoco, I. J. (1988) *Proc. Natl. Acad. Sci. U.S.A. 85*, 6252–6256.
Preston, B. D., Zakour, R. A., Singer, B., & Loeb, L. A. (1988) in *DNA Replication and Mutagenesis* (Moses, R. E., Summers, W. C., Eds.) American Society for Microbiology, Washington, D.C.
Radman, M., & Wagner, R. (1988) *Sci. Am. 259*, 24–30.
Saffhill, R., Margison, G. P., & O'Connor, P. J. (1985) *Biochim. Biophys. Acta 823*, 111–145.
Singer, B., Chavez, F., Goodman, M. F., Essigmann, J. M., & Dosanjh, M. K. (1989) *Proc. Natl. Acad. Sci. U.S.A. 86*, 8271–8274.
Smith, C. A., Xu, Y.-Z., & Swann, P. F. (1990) *Carcinogenesis 11*, 811–816.
Snow, E. T., Foote, R. S., & Mitra, S. (1984) *J. Biol. Chem. 259*, 8095–8100.
Sriram, M., van der Marel, G. A., Roelen, H. L. P. F., van Boom, J. H., & Wang, A. H.-J. *EMBO J. 11*, 225–232.
Sukumar, S. (1990) *Cancer Cells 2*, 199–204.
Swann, P. F. (1990) *Mutat. Res. 233*, 81–94.
Vadja, S., Valko, P., & Turanyi, T. (1985) *Int. J. Chem. Kinet. 17*, 55–81.
Wong, I., Patel, S. S., & Johnson, K. A. (1991) *Biochemistry 30*, 526–537.
Zarbl, H., Sukumar, S., Arthur, A. V., Martin-Zancar, D., & Barbacid M. (1985) *Nature 315*, 382–385.